MOLECULAR AND CELLULAR BIOLOGY, Oct. 1997, p. 6157–6166 Vol. 17, No. 10
0270-7306/97/$04.00+0

High-Resolution Analysis of DNA Replication Domain Organization across an R/G-Band Boundary

SABINE STREHL,[1] JANINE M. LASALLE,[1] AND MARC LALANDE[1,2]*

Genetics Division, Children's Hospital and Harvard Medical School,[1] and Howard Hughes Medical Institute,[2] Boston, Massachusetts 02115

Received 25 April 1997/Returned for modification 18 June 1997/Accepted 23 July 1997

Establishing how mammalian chromosome replication is regulated and how groups of replication origins are organized into replication bands will significantly increase our understanding of chromosome organization. Replication time bands in mammalian chromosomes show overall congruency with structural R- and G-banding patterns as revealed by different chromosome banding techniques. Thus, chromosome bands reflect variations in the longitudinal structure and function of the chromosome, but little is known about the structural basis of the metaphase chromosome banding pattern. At the microscopic level, both structural R and G bands and replication bands occupy discrete domains along chromosomes, suggesting separation by distinct boundaries. The purpose of this study was to determine replication timing differences encompassing a boundary between differentially replicating chromosomal bands. Using competitive PCR on replicated DNA from flow-sorted cell cycle fractions, we have analyzed the replication timing of markers spanning roughly 5 Mb of human chromosome 13q14.3/q21.1. This is only the second report of high-resolution analysis of replication timing differences across an R/G-band boundary. In contrast to previous work, however, we find that band boundaries are defined by a gradient in replication timing rather than by a sharp boundary separating R and G bands into functionally distinct chromatin compartments. These findings indicate that topographical band boundaries are not defined by specific sequences or structures.

Human metaphase chromosomes can be cytogenetically identified by a distinctive banding pattern that is achieved by different staining techniques. Chromosome banding using DNA-specific stains such as Giemsa and quinacrine was first described almost 30 years ago (42), and the most common banding types are now referred to as Giemsa (G) bands and reverse (R) bands. Despite significant advances in staining techniques, there has been little progress in understanding the underlying chromosomal structures responsible for the banding phenomenon.

R bands are characterized by early replication, high gene and CpG island density, and localization of a large number of both housekeeping and tissue-specific genes, and they are enriched for short interspersed repetitive elements. G bands are late replicating, contain a low number of tissue-specific genes, and are enriched for long interspersed repetitive elements (5, 6, 11, 19, 20, 31, 32). These general properties of R and G bands define them as distinct structural and functional units, suggesting the presence of discrete topographical boundaries. However, at higher levels of band resolution, it seems to be increasingly difficult to define narrow chromosome band boundaries, and the potential to correlate specific bands with specific functional sequences seems unlikely (19). Thus, to understand how the genome is organized in alternating chromosome bands and how boundaries between them are established, it is important to analyze functional differences between bands at the molecular level.

Chromosome replication in the eukaryotic cell nucleus is confined to a discrete portion of the cell cycle and is under stringent temporal and spatial control. Initiation of DNA replication occurs in coordinated groups of adjacent origins termed replicons (25, 45). Each replication domain represents a cluster of 10 to 20 replicons that synchronously initiate and terminate DNA synthesis, thus organizing the genome in a series of replication time bands (25, 32). Replication banding patterns that can be visualized by incorporation of 5′-bromodeoxyuridine (BrdU) in conjunction with differential staining techniques or by immunocytochemical methods exhibit an overall congruency with structural banding patterns (5, 11, 32). Several studies have determined the temporal order of replication domains and the correlation between changes in replication timing and gene expression over extensive regions of chromatin (26, 28, 37, 38, 50, 54, 55), but the correlation between replication timing domains and physical R/G-band boundaries remains unclear.

We have investigated the replication kinetics of the band boundary region between an early-replicating R band (13q14.3) and a late-replicating G band (13q21.1) of human chromosome 13. To determine the kinetics of DNA replication at high resolution, we have developed a competitive PCR-based assay that allows the determination of the replication time of single-copy DNA sequences in complex genomes. In this approach, cells in exponential growth are pulse-labeled with BrdU and fractionated by retroactive synchrony flow sorting into six cell cycle fractions based on their DNA content (21). Positive selection for replicated BrdU-substituted DNA is accomplished by immunoprecipitation with an anti-BrdU antibody (26, 27, 36, 56, 57). The amount of DNA in each cell cycle fraction is determined and can be calibrated by amplification of the BrdU-labeled mitochondrial DNA, since mitochondrial DNA replicates throughout the synthetic phase (2, 7). The replication kinetics of single-copy DNA sequences was analyzed by a competitive PCR method, similar to the approach that has been described for high-resolution mapping of origins of replication in mammalian cells (10, 14).

This approach allows the high-resolution delineation of replication timing at the transition zone between differentially

* Corresponding author. Mailing address: Genetics Division, Children's Hospital, 300 Longwood Ave., Boston, MA 02115. Phone: (617) 355-7387. Fax: (617) 355-7588. E-mail: lalande@rascal.med.harvard.edu.

replicating chromosomal bands. We have determined the replication timing of various genomic PCR markers termed sequence-tagged sites (STS), distributed over a continuous chromosome segment of about 4 to 5 Mb encompassing a proposed R/G-band boundary. In contrast to recent work suggesting a precise replication time switching and narrow band boundaries (55), our results indicate that at high resolution, replication is a dynamic process and that topographical band boundaries cannot be exactly defined on the basis of this functional property.

MATERIALS AND METHODS

Construction of cloned contigs. (i) YACs. To establish a yeast artificial chromosome (YAC) contig spanning the 13q14.3/q21.1 chromosomal band transition region, we screened the CEPH-Généthon YAC database for clones listed as positive for STSs D13S25, D13S31, and D13S59, which have been previously mapped into the vicinity of the proposed R/G-band boundary. YAC clones 857C5 (insert size of 1.6 Mb), 935G2 (1.7 Mb), 954C12 (2.2 Mb), 923F5 (1 Mb), 816D1 (1.4 Mb), and 850G8 (0.9 Mb) were obtained from Research Genetics (Huntsville, Ala.), and the sizes of the YACs were retrieved from the CEPH-Généthon database. Each clone was streaked onto selective agar plates, and DNA for PCR amplification was directly obtained from single colonies by boiling them in a YAC lysis solution (1% Triton X-100, 20 mM Tris [pH 8.5], 2 mM EDTA).

(ii) P1, PACs, and BACs. Bacteriophage P1, P1-derived artificial chromosomes (PACs), and bacterial artificial chromosomes (BACs) (35, 51, 53) were obtained commercially (Genome Systems, St. Louis, Mo.) by PCR screening the libraries with primers for markers D13S298 and D13S137. For contig assembly and the development of new PCR markers, terminal sequences of the clones were obtained by cloning the ends and fluorescent automated DNA sequencing (Applied Biosystems Inc., Foster City, Calif.). PCR primers were designed from the end clones containing single-copy sequences by using the Primer3 software (http://www-genome.wi.mit.edu/cgi-bin/primer/primer3.cgi). These primers were used to isolate new clones from different libraries.

Two nonoverlapping P1/PAC/BAC contigs around markers D13S298 and D13S137 consisting of six (Genome Systems control numbers P1 9532, P1 9533, PAC 10861, PAC 11350, PAC 12003, and PAC 12388) and three (PAC 11828, BAC 13636, and BAC 13637) clones were established. Overlaps among P1/PAC/BAC clones were determined by standard procedures, including PCR with appropriate STS primers, restriction fragment analysis, and pulsed-field gel electrophoresis (22).

Placement of markers on the physical map. PCRs for placement of STSs within the YAC and P1/PAC/BAC contigs were performed for markers RB-1 (exons 3 and 26 [60]), D13S818 (RBKPT), D13S165 (AFM203xa1), D13S319 (MGG15), D13S272 (AFM120xa3), D13S912 (WI-5710), D13S25 (H2-42), D13S262 (AFM205vh2), D13S294, D13S228, D13S31, D13S227 (CA20), D13S288 (AFM303zg5), D13S284, D13S268 (AFM238vc3), D13S295, D13S297, D13S788 (CHLC.GATA.P14583), D13S201 (MGG14), D13S301, D13S133, D13S300, D13S299, D13S298, D13S137, D13S155 (AFM070xb7), and D13S59. Primer sequences are available through the Genome Database (http://gdbwww.gdb.org/). Seven new STS markers, p752, p705, p702, p775, p838, p868, and p1027, were generated from P1/PAC/BAC clone end fragments. The chromosomal origin of each marker was verified by PCR amplification of two human × rodent cell hybrids: PGMEC8 containing a normal intact chromosome 13 and G46C2 carrying a 13;X translocated chromosome with region 13pter-13q22 retained (41). In addition, for positioning some STS deletion hybrid cell lines, CF25 (13q12-13qter), WC-H38B3B6 containing 13pter-q13::13q21.1-qter, and WC-H12D12 containing 13pter-q14::13q22-qter were used (33, 41). All PCRs were performed at least twice to verify reproducibility.

Cell culture and flow cytometry. Human lymphoblastoid cell lines GM7342 and GM7042 were cultured at 37°C in RPMI 1640 medium supplemented with 10 to 15% fetal calf serum (FCS) and penicillin-streptomycin (50 U/ml; Gibco BRL, Life Technologies, Gaithersburg, Md.). Human peripheral blood T lymphocytes (PBL) from healthy donors were isolated by Ficoll-Paque (Pharmacia Biotech, Uppsala, Sweden) gradient density centrifugation. The lymphocytes were stimulated by addition of phytohemagglutinin (1 μg/ml; Murex Diagnostics, Dartford, England) for about 60 h. To suppress endogenous thymidine synthesis, cells in exponential growth were treated with 25 μM fluorodeoxyuridine (Sigma, St. Louis, Mo.) for 15 min. Cells were centrifuged and resuspended in release medium (RPMI 1640 containing 10% dialyzed FCS [HyClone Laboratories, Inc., Utah] and 100 μM BrdU [Sigma]). Following a 45-min incubation at 37°C in the dark, cells were stained with 4′,6-diamidino-2-phenylindole (DAPI) and subjected to flow cytometry. Briefly, cells were resuspended in 1 ml of phosphate-buffered saline, and an appropriate amount of staining buffer (0.1 M Tris [pH 7.5], 146 mM NaCl, 0.2% FCS, 1 mM $CaCl_2$, 0.5 mM $MgCl_2$, 0.1% Nonidet P-40, 50 μg of RNase per ml, 2 μg of DAPI per ml) was added to yield a final cell concentration of about 10^6/ml (52). Cells were flow sorted based on their DNA content into six cell cycle fractions (G_1, S_1 to S_4, and G_2; 0.3×10^6 to 1×10^6 cells per fraction) on a FACS Vantage (Becton Dickinson) (21). Manipulations of labeled cells and DNA were done so as to avoid extensive exposure to light to prevent photolysis of incorporated BrdU.

DNA extraction and immunoprecipitation of BrdU-labeled DNA. DNA isolation was performed by standard procedures, and immunoprecipitation of BrdU-labeled DNA was carried out as described previously (26, 27, 36, 56, 57), with some modifications. Cells from each flow-sorted fraction were centrifuged, resuspended in extraction buffer (250 mM EDTA, 1% sarcosine, 200 μg of proteinase K per ml [pH 7.8]), and incubated for 16 h at 37°C. DNA from the lysates was extracted three times, twice with phenol-chloroform (1:1) and once with chloroform, ethanol precipitated, and rehydrated in 500 μl of 1 × TE (10 mM Tris [pH 7.5], 1 mM EDTA); 50 μg of high-molecular-weight salmon sperm DNA was added to each fraction. The DNA was sonicated for 15 to 30 s (Branson Sonifier 250), and the fragment sizes were determined by gel electrophoresis to range between 700 bp and 1.5 kb, with an average size of 1 kb. After heat denaturing and cooling on ice, samples were adjusted to 10 mM sodium phosphate (pH 7.0)–0.14 M NaCl–0.05% Triton X-100 and incubated with 1 μg of anti-BrdU antibody (Boehringer Mannheim, Indianapolis, Ind.). After 20 to 30 min of incubation in the dark at room temperature under mild shaking, an excess of a second antibody (30 μg of anti-mouse immunoglobulin G; Sigma) was added, and incubation continued for another 20 to 30 min. The precipitate was collected by 5 min of centrifugation. The pellets were washed in 500 μl of 10 mM sodium phosphate (pH 7.0)–0.14 M NaCl–0.05% Triton X-100, resuspended in 200 μl of 50 mM Tris (pH 7.8)–10 mM EDTA–0.5% sodium dodecyl sulfate–200 μg of proteinase K per ml, and incubated overnight at 37°C. After performing a second round of immunoprecipitation, starting with the addition of salmon sperm DNA, DNA was extracted and ethanol precipitated by adding glycogen (Boehringer Mannheim) or Pellet Paint Co-Precipitant (Novagen Inc., Madison, Wis.) to ensure the highest possible recovery of the BrdU-labeled immunoprecipitated DNA. The samples were resuspended in 50 to 80 μl of 1× TE and stored in the dark at 4°C. To control the different recovery during DNA extraction and immunoprecipitation, the concentration of DNA in each fraction was calibrated by PCR amplification of the BrdU-labeled mitochondrial DNA (mtDNA) in the samples. The PCR was performed in the linear range of the reaction, using primers MTRNA-1 (5′-GCCTTCCCCCGTAAATGATA-3′) and MTRNA-2 (5′-AACCACTTTCACCGCTACAC-3′), as follows: 94°C for 2 min; 25 cycles of 94°C for 30 s, 57°C for 30 s, and 72°C for 30 s; and a final extension at 72°C for 7 min. PCR products were visualized on agarose gels stained with ethidium bromide, gel images were captured by using a gel documentation system (ImageStore 5000; UVP, San Gabriel, Calif.), and band intensities were determined by using the GelBase/GelBlot Pro software (UVP).

Construction of PCR competitors and competitive PCR. For each locus and primer set, we constructed a competitor DNA segment consisting of a nonhomologous sequence 50 to 100 bp longer or shorter than the specific target sequence and having the same primer sequences. The competitors were constructed essentially as described in the protocol for the PCR MIMIC construction kit (Clontech Laboratories, Inc., Palo Alto, Calif.). Two rounds of PCR amplification were performed. In the first round, two composite primers, consisting of the target gene primer sequence attached to a 20-nucleotide stretch of a sequence designed to hybridize to opposite strands of a heterologous DNA fragment, were used. The desired primer sequences are thus incorporated during the PCR amplification. A dilution of the first PCR mixture is then amplified by using only the target-specific primers, ensuring that all competitor molecules contain the specific primer sequences. After purification by passage through Chroma-spin+TE-100 columns (Clontech), the concentration of competitor was calculated, and the competitor was diluted and used in the competitive PCR experiments.

Quantification and determination of replication timing. Competitive PCR experiments with the BrdU-substituted immunoprecipitated DNA of the six cell cycle fractions were carried out by adding various amounts of competitor to a fixed volume of the BrdU samples and amplifying the two targets simultaneously. PCRs were carried out in a total volume of 25 μl containing 0.5 to 1 μM each primer and 0.5 to 1 U of *Taq* (Boehringer Mannheim or Gibco BRL) in 10 mM Tris-HCl, 1 to 2 mM $MgCl_2$, 50 mM KCl, 25 μM each dATP, dCTP, dTTP, dGTP, and 2 to 5% dimethyl sulfoxide in some reactions. All PCRs were carried out in a GenAmp PCR System 2400 (Perkin-Elmer). After initial denaturing (94°C for 2 min) and amplification for 35 to 40 cycles (94°C for 30 s, 52 to 66°C for 30 s, 72°C for 30 s, and final extension at 72°C for 7 min), the two products were resolved by gel electrophoresis on 3% ethidium bromide-stained NuSieve agarose gels (FMC BioProducts, Rockland, Maine), and band intensities were determined by using the GelBase/GelBlot Pro software (UVP). Competitor DNA was added to achieve an approximately 1:1 ratio between competitor and BrdU-DNA (range of 0.3 to 5 for the BrdU-DNA) in the cell cycle fraction containing most of the replicated DNA. By setting the value for this particular cell cycle fraction as 100%, the percentage of relative replication of each time point for different markers was determined. The competitive PCR for each locus analyzed was repeated at least twice by adding different competitor concentrations to a fixed amount of BrdU-DNA.

Nucleotide sequence accession numbers. GenBank accession numbers for p752, p705, p702, p775, p838, p868, and p1027 are as follows: AF018661, AF018660, AF018659, AF018662, AF018663, AF018664, and AF018665, respectively.

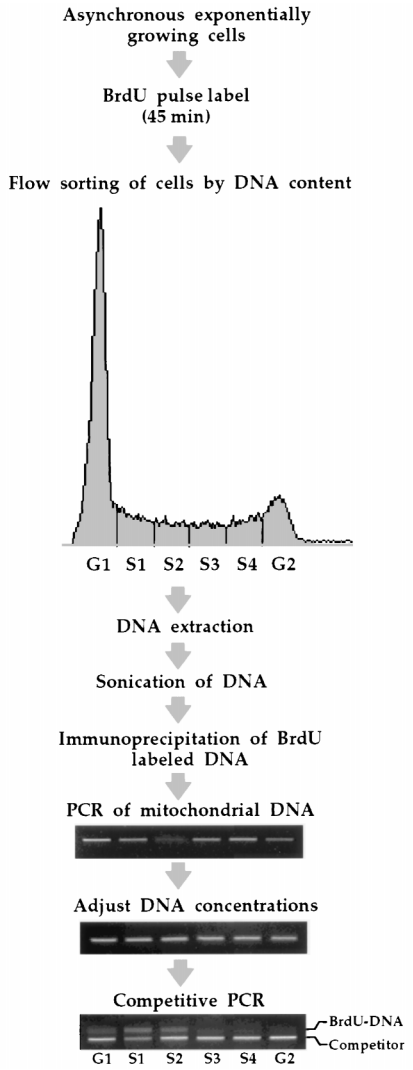

FIG. 1. Flow chart diagram showing the procedure for determination of replication timing. Following BrdU pulse-labeling, cells are flow sorted into six cell cycle fractions according to DNA content. After DNA extraction, the BrdU-substituted DNA of the six fractions is isolated by immunoprecipitation, and the DNA concentrations are adjusted by PCR using primers for mtDNA. For determination of replication timing, the calibrated samples are subjected to competitive PCR using locus-specific primers. An example for an early-replicating locus (D13S268) displaying a maximum of BrdU-DNA in S_1/S_2 is shown.

RESULTS

Establishment of a PCR assay for determination of replication timing. Lymphoblastoid cell lines or phytohemagglutinin-stimulated lymphocytes in exponential growth were pulse-labeled with BrdU for 45 min and fractionated into six cell cycle phases (21), G_2/M (mitotic), G_1, and four synthetic (S)-phase fractions, by flow cytometry (Fig. 1). For each flow sorting experiment, the gates were set in exactly the same way and equal numbers of cells, ranging from 0.3×10^6 to 1×10^6, were acquired for each fraction of the cell cycle. Purification of the replicated BrdU-substituted DNA was achieved by immunoprecipitation with an anti-BrdU antibody (26, 27, 36, 56, 57). In previous studies, PCR of flow-sorted cell cycle fractions after negative (52) or positive (26, 27, 36) selection of BrdU-substituted DNA has been used to study replication kinetics. Flow sorting does not require cell synchronization steps using metabolic inhibitors and eliminates any potential of cell cycle perturbation (21). Positive selection of BrdU-substituted DNA by immunoprecipitation may result in different recovery of the replicated DNA. Since replication of mtDNA is not linked to nuclear DNA synthesis and may occur at any time during the cell cycle (2, 7), the concentration of DNA in each fraction was calibrated by PCR amplification of the BrdU-labeled mtDNA contained in the samples. The high abundance of mtDNA allowed the PCR to be performed in the linear range of amplification (25 cycles) and to visualize the amplified products on ethidium bromide-stained agarose gels. After quantification of the band intensities, the DNA concentrations of the samples were adjusted and again subjected to PCR amplification. In general, this procedure had to be carried out for one to two rounds to achieve equal band intensities with the mtDNA primers (Fig. 1).

The replication timing for a particular locus was analyzed by competitive PCR of the calibrated cell cycle-fractionated DNA by using locus-specific primers. A similar method has been described for high-resolution mapping of origins of replication in mammalian cells (10, 14). In our approach, a nonhomologous competitor sharing the locus-specific primer sequences was constructed and then amplified simultaneously with the BrdU samples as an internal control for the efficiency of the PCR. The size differences between the two products allowed their resolution and direct visualization by gel electrophoresis on ethidium bromide-stained agarose gels (Fig. 1). Various concentrations of competitor DNA were added to a fixed amount of replicated DNA to achieve an approximately 1:1 ratio of the amplification products in the fractions containing the highest amounts of BrdU-substituted DNA. The replication time of each locus was derived from at least two independent competitive PCR experiments using different concentrations of competitor and by calculating the ratios between competitor and the specific target (for details, see Materials and Methods). In most cases, PCR amplification of the replicated BrdU-substituted DNA without using the competitor resulted in specific amplification of the same cell cycle fractions as after competitive PCR (data not shown), thus confirming the highly efficient enrichment of replicated DNA. As size and nucleotide differences of PCR targets can influence amplification rates (61), we used the competitor fragments to control for amplification anomalies and to compare the relative rather than the absolute amounts of replicated sequences in the different cell cycle fractions.

To demonstrate that our method is comparable to other techniques measuring replication timing, we determined the replication pattern of β2-microglobulin (β2-MG) (52) and FMR1 on the X chromosome (26, 28, 54). β2-MG showed a very early replication pattern (Fig. 2A) which is consistent with the finding that this gene starts replicating 2 to 4 h after release from the G_1/S boundary in cell synchronization experiments (52). In normal male lymphocytes, FMR1 showed a mid-to-late replication pattern (Fig. 2B), thus confirming the replication pattern of this locus previously established by using alternative methods for measuring replication timing (26, 28, 54).

To test the reproducibility of the assay, we determined the replication timing of selective markers by using various competitor DNA concentrations and immunoprecipitated DNA from independent cell sorts. Representative examples of these experiments are shown in Fig. 3A and B. Different BrdU-DNA/competitor ratios, ranging between 0.3:1 and 5:1, did not significantly influence the calculation of percentage of relative replication for an individual locus. In addition, the replication kinetics of selected markers in assays using BrdU-DNA from

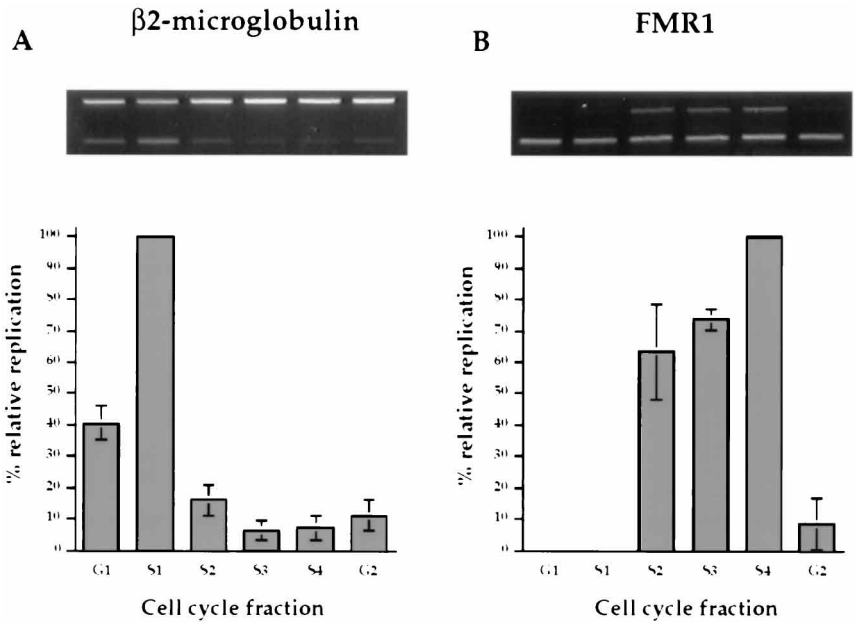

FIG. 2. Determination of replication timing of β2-MG (A) and FMR1 (B). β2-MG shows a very early replication pattern; FMR1 shows a mid-to-late pattern. Results in the histograms are expressed as means and standard deviations (error bars) of four independent competitive PCRs using different competitor concentrations and resulting in BrdU-DNA/competitor ratios ranging from 0.2:1 to 5:1 in S_1 for β2-MG (A) and three experiments (BrdU-DNA/competitor ratios of 0.35:1 to 0.6:1) in S_4 for FMR1 (B).

independent cell sorts was reproducible, demonstrating the reliability of the assay (Fig. 3C and D).

Construction of a contig map of 13q14.3-q21.1. To demonstrate a correlation between replication timing and structural band boundaries, we have constructed a high-resolution physical map spanning the 13q14.3-q21.1 chromosomal band transition region. YACs were obtained after screening the CEPH-Généthon database for YACs containing markers D13S25, D13S31, and D13S59. Overlaps among the YACs were determined by YAC STS content as assayed by PCR amplification. The YAC contig consisting of YACs 857C5 (1.6 Mb), 935G2 (1.7 Mb), 954C12 (2.2 Mb), 923F5 (1 Mb), 816D1 (1.4 Mb), and 850G8 (0.9 Mb) covers a continuous segment of chromosome 13 spanning about 3 to 4 Mb between D13S272 and D13S59 and extends an undetermined distance beyond these markers (Fig. 4).

Twenty-three previously established and seven new single-copy PCR markers (see Materials and Methods) were localized within the YAC contig. Three markers, RB-1, D13S818, and D13S165, are proximal of the contig, while D13S288 is distal. The order of markers presented in Fig. 4 is based on the physical map established at the Third International Workshop on Human Chromosome 13 Mapping (58) and on other maps of the 13q14 region (4, 29, 30, 40, 44, 59). Marker placement around the proposed R/G-band boundary also depended on the analysis of two nonoverlapping P1/PAC/BAC contigs established in this chromosomal region around STSs D13S298 and D13S137 (Fig. 4). Markers D13S299 and D13S300 are physically localized within an overlapping cosmid contig (44); consequently, the two contigs are roughly separated by a maximal distance of 200 kb. The approximate distances between markers were estimated from the sizes of the YAC clones, analysis of the two P1/PAC/BAC contigs (Fig. 4), and data taken from previous studies (3, 30, 44). D13S288 was mapped distal to the YAC contig, but the physical distance could not be determined.

Determination of the temporal order of replication. The replication kinetics of a number of STSs spanning the proposed R/G-band transition zone between the differentially replicating chromosomal bands 13q14.3 and 13q21.1 was determined. The Wilson disease locus, which is tightly linked to D13S31, has been physically mapped to the junction of bands 13q14.3 and 13q21.1 by fluorescence in situ hybridization (39), thus giving us a starting point for our investigations. In initial experiments, we determined the replication timing of D13S31 and markers distal and proximal of this locus. All proximal markers, including RB-1 and D13S25, separated from D13S31 by distances of about 2 Mb and at least 500 kb, respectively, showed an early replication pattern with maxima in S_1 and/or S_2. D13S59, localized 2 to 3 Mb distal of D13S31, showed a strikingly different very late replication pattern (S_4/G_2), indicating that a switch in replication timing must occur between D13S31 and D13S59 (Fig. 5A to C). The replication observed in G_2 (Fig. 5C) can be explained by very late replication events that overlap the G_2 fraction in the flow sorting procedure.

To narrow down the region where this change in replication timing appears, we further analyzed the replication kinetics of a number of DNA sequences encompassing the interval between D13S31 and D13S59. As this high-resolution analysis progressed, it became apparent that the replication timing progressively shifted from very early (e.g., RB1 and D13S25) to mid (D13S137), and finally to very late (D13S155 and D13S59) S-phase replication, indicating that we had indeed crossed the band boundary (Fig. 4). Surprisingly, we observed a gradient of replication timing over an extensive (1- to 2-Mb) region rather than an abrupt change one would expect if R and G bands represent distinct chromosome replication timing and structural domains.

To confirm and extend these results, we determined the replication timing within a chromosome segment of about 1 Mb that spanned more than 500 kb from the late-replicating STSs D13S155 and D13S59 into the more proximal earlier-

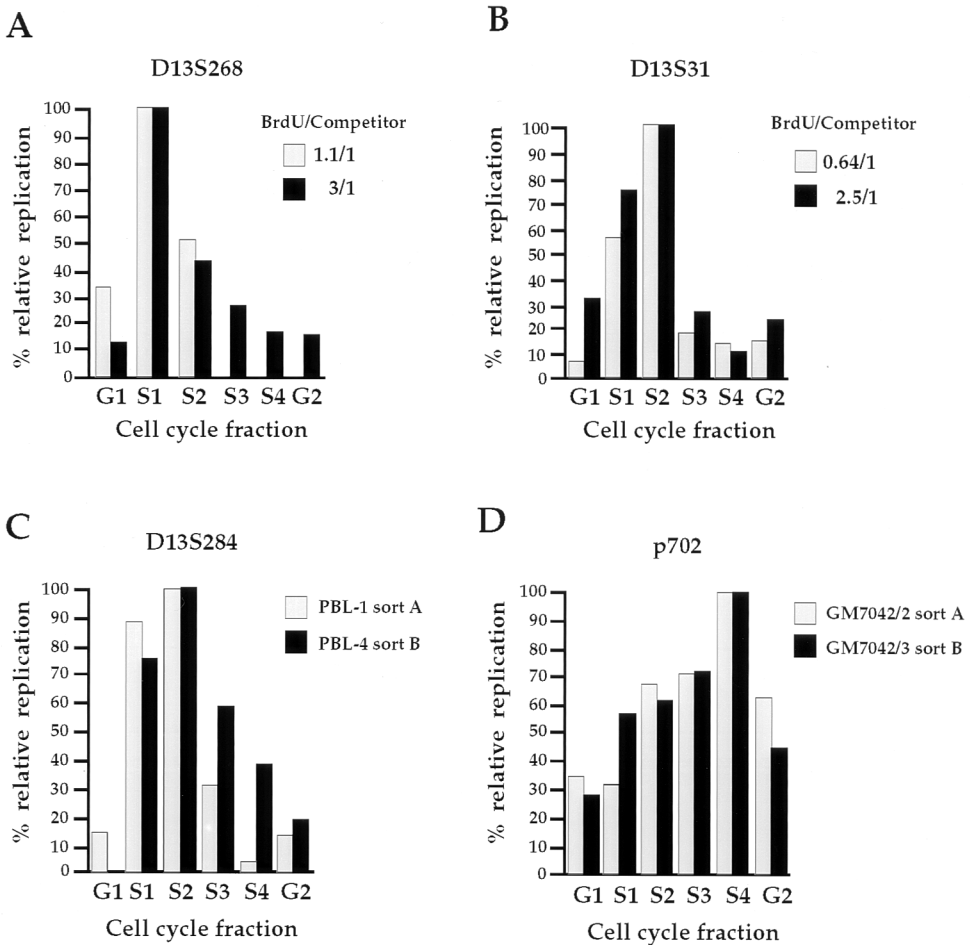

FIG. 3. Quantification of competitive PCRs testing the influence of the amounts of competitor DNA added on the percentage of relative replication (A and B) and comparison of results obtained from independent cell sorts (C and D). Two independent competitive PCRs using different amounts of competitor and a fixed amount of BrdU-DNA from the same cell sorting experiment were performed for markers D13S268 (A) and D13S31 (B). Different BrdU-DNA/competitor ratios did not significantly influence the determined maxima of replication for a particular locus. Competitive PCRs for D13S284 (C) and p702 (D) were performed on BrdU-DNA from independent cell sorts of two lymphocyte cultures (C) and two flow sorting experiments using lymphoblastoid cells (D). The determination of replication kinetics in assays using BrdU-DNA derived from independent cell sorts produced the same results.

replicating domain. Within this domain, some markers (p868 and p1027) displayed an S_3/S_4 replication pattern and were flanked by markers showing S_2/S_3 (p702 and p838) and S_4/G_2 (D13S155 and D13S59) patterns localized proximal and distal, respectively (Fig. 4). Examples of competitive PCRs demonstrating the different replication patterns within the band boundary region are shown in Fig. 5D to F. These data confirmed the observations that the R/G-band boundary is characterized by a gradual shift in replication timing. Including the RB-1 gene as the most proximal and D13S59 as the most distal marker, we have determined the replication timing over a continuous chromosome region encompassing a physical distance of 4 to 5 Mb and crossing the R/G-band junction region. The replication times of all STSs analyzed in PBL and their roughly estimated physical distances are summarized in Fig. 4.

Replication timing in different cultured mammalian cells. A shift toward later replication, which corresponds to about one cell cycle fraction, was observed in Epstein-Barr virus (EBV)-transformed lymphoblasts relative to PBL for markers showing intermediate replication patterns (Fig. 6). Preliminary data on the replication kinetics of the same sequences in fibroblasts (data not shown) indicate a pattern similar to that of PBL rather than that of lymphoblasts. For very early (S_1/S_2)- and the very late (S_4/G_2)-replicating sequences, no significant differences in replication timing in the different tissues were observed. Despite these slight differences between PBL and lymphoblasts, the temporal order of replication remained unchanged.

DISCUSSION

The comparison of morphological banding to replication banding suggests a close relationship between the structure and function of chromosome bands (11). There have been few studies regarding the underlying complexity of chromatin organization and the functional differences determining domain organization and topographical boundaries at the molecular level (55). The results of our high-resolution replication kinetic analysis of the chromosome 13q14.3/q21.1 band boundary region indicate that the timing of replication gradually shifts from early to late over a several-megabase-pair region. These data are inconsistent with R and G bands being partitioned into replication timing domains separated by distinct and definable boundaries.

Previous molecular studies of chromosome bands have mainly been concerned with the differential AT or GC base

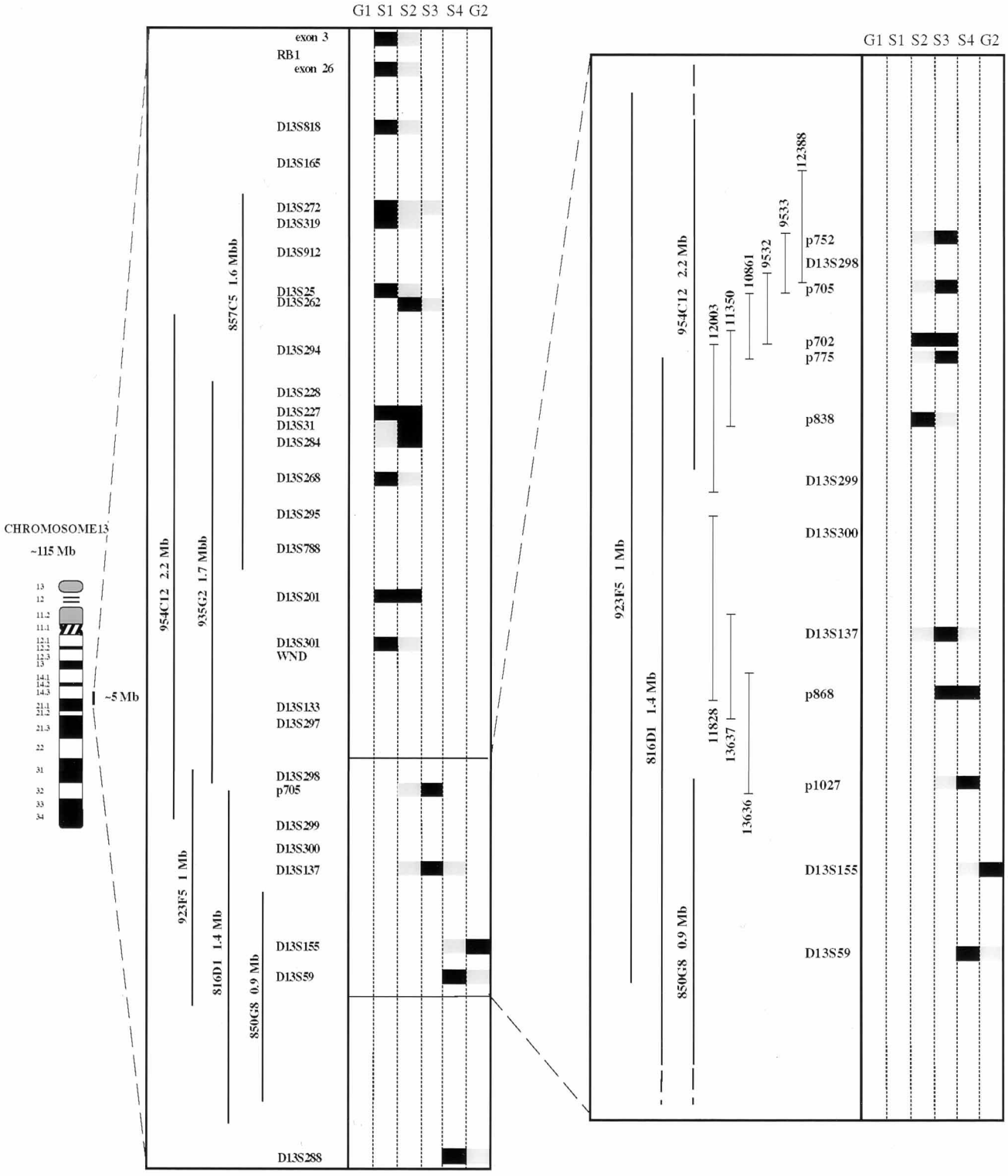
G1 S1 S2 S3 S4 G2
exon 3
RB1
exon 26
D13S818
D13S165
D13S272
D13S319
D13S912
D13S25
D13S262
D13S294
D13S228
D13S227
D13S31
D13S284
D13S268
D13S295
D13S788
D13S201
D13S301
WND
D13S133
D13S297
D13S298
p705
D13S299
D13S300
D13S137
D13S155
D13S59
D13S288
857C5 1.6 Mbb
954C12 2.2 Mb
935G2 1.7 Mbb
923F5 1 Mb
816D1 1.4 Mb
850G8 0.9 Mb
CHROMOSOME13
~115 Mb
~5 Mb
G1 S1 S2 S3 S4 G2
954C12 2.2 Mb
923F5 1 Mb
816D1 1.4 Mb
850G8 0.9 Mb
12388
9533
9532
10861
11350
12003
11828
13637
13636
p752
D13S298
p705
p702
p775
p838
D13S299
D13S300
D13S137
p868
p1027
D13S155
D13S59

FIG. 4. Determination of replication kinetics and high-resolution physical map across the R/G-band boundary of differentially replicating chromosomal bands 13q14.3 and 13q21.1. The order and distances of 35 markers were determined to allow accurate comparison between physical localization and replication. The determined differences in replication timing in PBL showed that the R/G-band boundary is characterized by a gradual shift in replication timing. More detailed analysis of the replication patterns at the R/G-band transition is shown on the right panel. Cell cycle fractions displaying maxima of replicated BrdU-substituted DNA are shaded; the highest fractions are shown in dark shading, and the second-highest fractions are shown in light shading. If the differences of the values between two cell cycle fractions were less than 15%, the fractions are shown in the same shading. The replication pattern for each individual locus was determined after careful quantification of at least two independent competitive PCRs using different competitor concentrations and a fixed amount of BrdU-DNA.

content of R and G bands based on the data from conventional chromosome banding techniques suggesting that R bands are more GC rich than G bands (11, 31, 32, 49). This differential base content of R and G bands has been confirmed to some extent at the molecular level and has led to the isochore model of chromosome organization. This model describes the mammalian genome as a long-range G+C% mosaic structure that shows close relation to chromosome bands (46), and G-band DNA was found to be richer in AT than R-band DNA (5, 11, 32). However, this relatively minor long-range variation in base composition cannot satisfactorily explain chromosome banding (48). Cloning of sequences at putative isochore boundaries showed strong homology to the pseudoautosomal boundary sequences on the short arms of the sex chromosomes (17, 18). These sequences are transcribed (18), but their function and relationship to AT-GC isochores and/or R- and G-band boundaries remain unclear. Although there seems to be an overall correlation between isochore class, gene density, and banding patterns (46, 47, 62), sequences of very different G+C content are replicated simultaneously during S phase, and there appears to be no relationship between replication time and isochore class (13).

Our data are inconsistent with several investigations suggesting that, at the band level, R- and G-zone replication patterns are mutually exclusive (11, 16). These studies suggest a distinct cessation or reduction of DNA synthesis between completion of R-band replication and the commencement of G-band replication, implying that R and G bands represent different compartments of distinct chromatin activity. However, in unsynchronized cell populations, no cessation of DNA synthesis was observed, and it was suggested that for a short period of time, replication activity may be found in both band types (1). The wide usage of blocking agents that possibly generate an artificial synchrony might be responsible for these controversial observations. Our experimental approach in unsynchronized cells permits the analysis of replication timing domains at an R/G boundary, where the flanking G band is known to be one of the very late replicating bands in the human genome. It seems likely, therefore, that the change in replication timing at other band junctions will be even less obvious. These data support the idea that replication is continuous throughout S phase and is inconsistent with the postulate of a clean partition between R- and G-band replication and complete cessation of DNA synthesis at the R/G replication junction.

An alternative explanation for our observations is that there is a precise replication timing switch within each cell, but this boundary is different from cell to cell within a population. While there are variations in replication timing between individual cells, each flow-sorted S-phase fraction corresponds to about 2 h of the S-phase traverse time. Thus, for the differences that we observe to be due to cellular heterogeneity, cell-to-cell differences in the R/G-band transition would need to be very large, corresponding to about 25% of the S-phase duration. In addition, replication in more than one S-phase fraction is observed for markers not only from the mid but also from early and late replication domains, suggesting that cell heterogeneity affects replication timing equally throughout the cell cycle. This would argue against cellular heterogeneity solely accounting for the differences in replication timing of the R/G-band transition.

The number and pattern of expression of genes correlate with other features of chromosome bands (6, 31, 62), and transcriptional activity is associated with early replication (9, 12, 37, 50). At low resolution, widely expressed (housekeeping) genes and many tissue-specific genes are localized in the overall early replicating R bands (6, 19, 31); however, nothing is known about their distribution within a domain. We have preliminary evidence that housekeeping genes like RB-1 and the Wilson disease gene reside in the very early replicating domains, whereas highly tissue specific genes probably are localized in the R/G-band boundary regions displaying mid replication patterns. The close correlation between developmentally regulated gene expression and changes in replication timing (9, 12, 37, 50) may, thus, suggest that band boundaries are dynamic rather than precisely determined by specific DNA structures or sequences.

In a recent attempt to characterize a band boundary at the molecular level, a precise switch in replication timing was observed in the human major histocompatability complex (MHC) locus (55). In contrast to our findings, these data suggest a

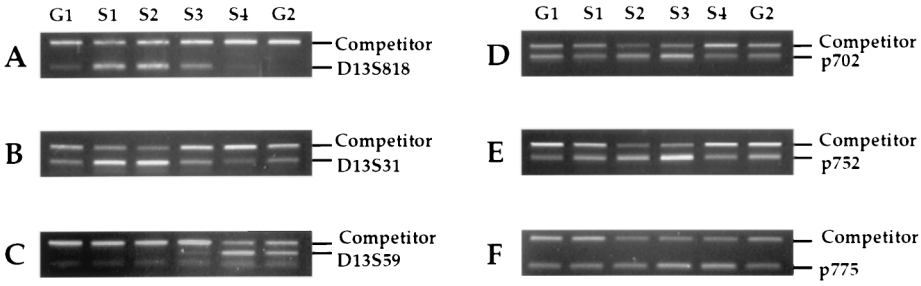

FIG. 5. Competitive PCRs showing different patterns of replication timing. (A and B) Early replication, displaying the highest amounts of amplified BrdU-DNA in cell cycle fractions S_1/S_2 (D13S818 and D13S31). (C) Late replication pattern with maximum replication in S_4/G_2 (D13S59). (D to F) Examples of intermediate replication patterns of loci localized at the R/G-band boundary. The replication timing of markers p702 and p752 was determined by using PBL BrdU-DNA; that of p775 was determined by using lymphoblastoid DNA.

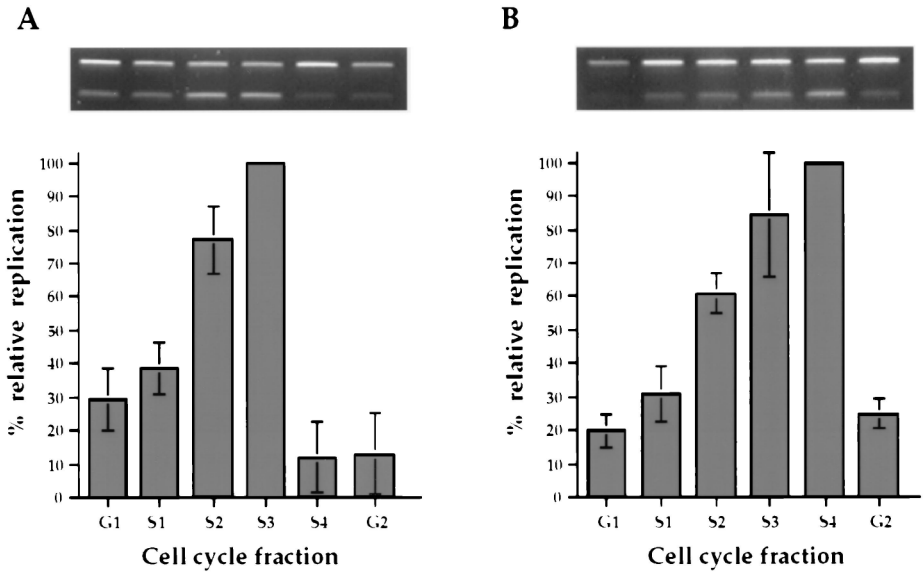

FIG. 6. Replication timing differences between PBL and EBV-transformed lymphoblastoid cell lines for locus p775. Lymphoblasts (B) display a shift toward later replication compared to lymphocytes (A). Results in the histograms are expressed as means and standard deviations (error bars) of two independent competitive PCRs.

narrow R/G-band transition. In some respects, these data are consistent with our model that band boundaries are dynamic in that a gradient in replication timing is also observed in the case of the MHC. In the latter case, this region extends only over 50 kb (55), while this region is about 1,000 kb in the 13q14.3/q21.1 transition zone. While this could reflect differences between the sizes of distinct band boundaries, another possibility is that boundaries also vary in different tissues, depending on the pattern of expression of the genes in and around such band transition regions. It should also be noted that the precise transition described (55) was determined by using cell synchronization and quantification of nascent DNA not allowing a direct comparison with the data obtained in this study. In addition, the study of replication timing in the MHC locus used the myeloid leukemia cell line HL60 rather than primary lymphocytes, making direct comparison with our data somewhat difficult. Finally, switches in replication timing within fairly short distances have been described by several investigators (12, 37, 38, 50) and do not necessarily correspond to chromosomal band boundaries.

The analysis of the replication timing domains in different tissues showed that in EBV-transformed lymphoblastoid cells, the overall replication time is slightly delayed compared to PBL and fibroblasts. Although the precise replication time differed between PBL and lymphoblasts, the temporal ordering remained unchanged. The close relationship between gene expression and replication timing (9, 12, 37, 50) might account for these differences. In addition, the EBV genome integrates into the host DNA of the artificially immortalized cell lines, and it has been demonstrated that chromosome 13 contains integration hot spots in 13q13, 13q21, and 13q33 (43). However, to date the replication status of the integrated virus is not known, and it remains to be verified that the integrated virus can in fact influence the replication timing of adjacent host sequences. Although these differences in replication timing between PBL and lymphoblasts have not been found to affect the temporal order of replication within a domain, delayed replication in some domains might influence the delineation of timing zones.

Our findings may also have important implications for the studies of mammalian origins of chromosome replication. A homogeneous replication time for the entire extent of the R band would suggest the coordinate regulation of a group of origins contained within a 5- to 10-Mb stretch of DNA. The results summarized in Fig. 4 demonstrate that the 13q14.3 R band is, in fact, divided into several sequential domains of replication time, suggesting that origins are grouped into temporal domains corresponding to 500 to 1,000 kb of chromosomal DNA. This observation would be consistent with a relatively synchronous activation of early S-phase origins in the proximal region of 13q14.3. This event would then be followed by activation of origins in the more distal domains. These results suggest that both individual origins and groups of origins can be activated at different times in S phase, implying that mammalian chromosome replication is controlled at two levels. At one level, there is control of replication time for a cluster of origins, and the replication time of these domains can vary depending on chromosomal location. At another level within the domains, the replication time of individual origins is coordinately regulated. These assumptions are supported by work done on yeast chromosomes, in that the isolation of a temporally regulated origin suggests that origins are activated not just at the beginning of S phase but possibly throughout S (15). The time of replication of this origin is regulated by position, indicating that the time at which an origin is activated can depend on chromosomal context. While there has been considerable progress in the identification of individual origins (8, 15, 23, 24, 34), much remains to be learned about the regulation of origin clusters and, eventually, the mechanism of replication banding. The studies reported here represent a first step to the understanding of chromosome replication time domain organization and replication banding at the molecular level.

ACKNOWLEDGMENTS

We are grateful to Alan Flint for expert technical assistance with flow sorting, to Serge Anselem for the mtDNA primers, and to Webster Cavenee, Gail Bruns, and John Cowell for somatic cell hybrids.

This work was supported by a postdoctoral research grant from the

Max Kade Foundation to S.S., the NIH (grant P01-HD18658), and the Howard Hughes Medical Institute.

REFERENCES

1. **Aghamohammadi, S. Z., and J. R. K. Savage.** 1990. BrdU pulse/reverse staining protocols for investigating chromosome replication. Chromosoma (Berlin) **99:**76–82.
2. **Bogenhagen, D., and D. A. Clayton.** 1977. Mouse L cell mitochondrial DNA molecules are selected randomly for replication throughout the cell cycle. Cell **11:**719–727.
3. **Bull, P. C., and D. W. Cox.** 1993. Long range restriction mapping of 13q14.3 focused on the Wilson disease region. Genomics **16:**593–598.
4. **Bullrich, F., M. L. Veronese, S. Kitada, J. Jurlander, M. A. Caligiuri, J. C. Reed, and C. M. Croce.** 1996. Minimal region of loss at 13q14 in B-cell chronic lymphocytic leukemia. Blood **88:**3109–3115.
5. **Craig, J. M., and W. A. Bickmore.** 1993. Chromosome bands—flavours to savours. Bioessays **15:**349–354.
6. **Cross, S. H., and A. P. Bird.** 1995. CpG islands and genes. Curr. Opin. Genet. Dev. **5:**309–314.
7. **Davis, A. F., and D. A. Clayton.** 1996. In situ localization of mitochondrial DNA replication in intact mammalian cells. J. Cell Biol. **135:**883–893.
8. **DePamphilis, M. I.** 1993. Origins of DNA replication in metazoan chromosomes. J. Biol. Chem. **268:**1–4.
9. **Dhar, V., A. I. Skoultchi, and C. L. Schildkraut.** 1989. Activation and repression of a beta-globin gene in cell hybrids is accompanied by a shift in its temporal replication. Mol. Cell. Biol. **9:**3524–3532.
10. **Diviacco, S., P. Norio, L. Zentilin, S. Menzo, M. Clementi, G. Biamonti, S. Riva, A. Falaschi, and M. Giacca.** 1992. A novel procedure for quantitative polymerase chain reaction by coamplification of competitive templates. Gene **122:**313–320.
11. **Drouin, R., J. P. Holmquist, and C.-L. Richer.** 1994. High-resolution replication bands compared to morphologic G- and R-bands. Adv. Hum. Genet. **22:**47–115.
12. **Epner, E., W. C. Forrester, and M. Groudine.** 1988. Asynchronous DNA replication within the human β-globin gene locus. Proc. Natl. Acad. Sci. USA **85:**8081–8085.
13. **Eyre-Walker, A.** 1992. Evidence that both G+C rich and G+C poor isochores are replicated early and late in the cell cycle. Nucleic Acids Res. **20:**1497–1501.
14. **Falaschi, A., M. Giacca, L. Zentilin, P. Norio, S. Diviacco, D. Dimitrova, S. Kumar, R. Tuteja, G. Biamonti, G. Perini, F. Weighardt, J. Brito, and S. Riva.** 1993. Searching for replication origins in mammalian DNA. Gene **135:**125–135.
15. **Fangman, W. L., and B. J. Brewer.** 1992. A question of time: replication origins of eukaryotic chromosomes. Cell **71:**363–366.
16. **Fetni, R., R. Drouin, C.-L. Richer, and N. Lemieux.** 1996. Complementary replication R- and G-band patterns induced by cell blocking at the R-band/G-band transition, a possible regulatory checkpoint within the S phase of the cell cycle. Cytogenet. Cell Genet. **75:**172–179.
17. **Fukagawa, T., K. Sugaya, K. Matsumoto, K. Okumura, A. Ando, H. Inoko, and T. Ikemura.** 1995. A boundary of long-range G+C% mosaic domains in the human MHC locus: pseudoautosomal boundary-like sequence exists near the boundary. Genomics **25:**184–191.
18. **Fukagawa, T., Y. Nakamura, K. Okumura, M. Nogami, A. Ando, H. Inoko, N. Saitou, and T. Ikemura.** 1996. Human pseudoautosomal boundary-like sequences: expression and involvement in evolutionary formation of the present-day pseudoautosomal boundary of human sex chromosomes. Hum. Mol. Genet. **5:**23–32.
19. **Gardiner, K.** 1995. Human genome organization. Curr. Opin. Genet. Dev. **5:**315–322.
20. **Gardiner, K.** 1996. Base composition and gene distribution: critical patterns in mammalian genome organization. Trends Genet. **12:**519–524.
21. **Gilbert, D. M., and S. N. Cohen.** 1987. Bovine papilloma virus plasmids replicate randomly in mouse fibroblasts throughout S phase of the cell cycle. Cell **50:**59–68.
22. **Glatt, K., H. Glatt, and M. Lalande.** 1997. Structure and organization of GABRB3 and GABRA5. Genomics **41:**63–69.
23. **Hamlin, J. L.** 1992. Mammalian origins of replication. Bioessays **14:**651–659.
24. **Hamlin, J. L., and P. A. Dijkwel.** 1995. On the nature of replication origins in higher eukaryotes. Curr. Opin. Genet. Dev. **5:**153–161.
25. **Hand, R.** 1975. Regulation of DNA replication on subchromosomal units of mammalian cells. J. Cell Biol. **64:**89–97.
26. **Hansen, R. S., T. K. Canfield, M. M. Lamb, S. M. Gartler, and C. D. Laird.** 1993. Association of fragile X syndrome with delayed replication of the FMR1 gene. Cell **73:**1403–1409.
27. **Hansen, R. S., T. K. Canfield, and S. M. Gartler.** 1995. Reverse replication timing for the XIST gene in human fibroblasts. Hum. Mol. Genet. **4:**813–820.
28. **Hansen, R. S., T. K. Canfield, A. D. Fjeld, S. Mumm, C. D. Laird, and S. M. Gartler.** 1997. A variable domain of delayed replication in FRAXA fragile X chromosomes: X inactivation-like spread of late replication. Proc. Natl. Acad. Sci. USA **94:**4587–4592.
29. **Hawthorn, L. A., and J. K. Cowell.** 1995. Integration of the physical and genetic linkage map for human chromosome 13. Genomics **27:**399–404.
30. **Hawthorn, L. A., T. Roberts, E. Verlind, R. F. Kooy, and J. K. Cowell.** 1995. A yeast artificial chromosome contig that spans the RB1-D13S31 interval on human chromosome 13 and encompasses the frequently deleted region in B-cell chronic lymphocytic leukemia. Genomics **30:**425–430.
31. **Holmquist, G. P.** 1989. Evolution of chromosome bands: molecular ecology of noncoding DNA. J. Mol. Evol. **28:**469–486.
32. **Holmquist, G. P.** 1992. Chromosome bands, their chromatin flavors, and their functional features. Am. J. Hum. Genet. **51:**17–37.
33. **Houwen, R. H. J., S. E. Pautler, J. A. Barwell, K. Arden, J. A. Buchanan, C. D. James, W. K. Cavanee, C. H. C. M. Buys, J. K. Cowell, and D. W. Cox.** 1991. Isolation and regional localization of 25 anonymous DNA probes on a chromosome 13 hybrid panel. Cytogenet. Cell Genet. **57:**87–90.
34. **Huberman, J. A.** 1995. Prokaryotic and eukaryotic replicons. Cell **82:**535–542.
35. **Ioannou, P. A., C. T. Amemiya, J. Garnes, P. M. Kroisel, H. Shizuya, C. Chen, M. A. Batzer, and P. J. de Jong.** 1994. A new bacteriophage P1-derived vector for the propagation of large human DNA fragments. Nat. Genet. **6:**84–89.
36. **Kawame, H., S. M. Gartler, and R. S. Hansen.** 1995. Allele-specific replication timing in imprinted domains: absence of asynchrony at several loci. Hum. Mol. Genet. **4:**2287–2293.
37. **Kitsberg, D., S. Selig, I. Keshet, and H. Cedar.** 1993. Replication structure of the human β-globin gene domain. Nature **366:**588–590.
38. **Kitsberg, D., S. Selig, M. Brandeis, I. Simon, I. Keshet, D. J. Driscoll, R. D. Nicholls, and H. Cedar.** 1993. Allele-specific replication timing of imprinted gene regions. Nature **364:**459–463.
39. **Kooy, R. F., A. Y. Van der Veen, E. Verlind, R. H. J. Houwen, H. Scheffer, and C. H. C. M. Buys.** 1993. Physical localisation of the chromosomal marker D13S31 places the Wilson disease locus at the junction of bands q14.3 and q21.1 of chromosome 13. Hum. Genet. **91:**504–506.
40. **Kooy, R. F., A. Wijngaard, E. Verlind, H. Scheffer, and C. H. C. M. Buys.** 1995. An integrated map of human chromosome 13 allowing regional localization of genetic markers. Eur. J. Hum. Genet. **3:**180–187.
41. **Lalande, M., T. P. Dryja, R. R. Schreck, J. Shipley, A. Flint, and S. A. Latt.** 1984. Isolation of human chromosome 13-specific DNA sequences cloned from flow sorted chromosomes and potentially linked to the retinoblastoma locus. Cancer Genet. Cytogenet. **13:**283–295.
42. **Latt, S. A.** 1976. Optical studies of metaphase chromosome organization. Annu. Rev. Biophys. Bioeng. **5:**1–37.
43. **Lestou, V. S., M. De Braekeleer, S. Strehl, G. Ott, H. Gadner, and P. F. Ambros.** 1993. Non-random integration of Epstein-Barr virus in lymphoblastoid cell lines. Genes Chromosomes Cancer **8:**38–48.
44. **Petrukhin, K., S. G. Fischer, M. Piratsu, R. E. Tanzi, I. Chernov, M. Devoto, L. M. Brzustowicz, E. Cayanis, E. Vitale, J. J. Russo, D. Matseoane, B. Boukhgalter, W. Wasco, A. L. Figus, J. Loudianos, A. Cao, I. Sternlieb, O. Evgrafov, E. Parano, L. Pavone, D. Warburton, J. Ott, G. K. Penchaszadeh, I. H. Scheinberg, and T. C. Gilliam.** 1993. Mapping, cloning and genetic characterization of the region containing the Wilson disease gene. Nat. Genet. **5:**338–343.
45. **Rivin, C. J., and W. L. Fangman.** 1980. Replication fork rate and origin activation during the S phase of Saccharomyces cerevisiae. J. Cell Biol. **85:**108–115.
46. **Saccone, S., A. De Sario, J. Wiegant, A. K. Raap, G. Della Valle, and G. Bernardi.** 1993. Correlation between isochores and chromosomal bands in the human genome. Proc. Natl. Acad. Sci. USA **90:**11929–11933.
47. **Saccone, S., S. Caccio, J. Kusuda, L. Andreozzi, and G. Bernardi.** 1996. Identification of the gene-richest bands in human chromosomes. Gene **174:** 85–94.
48. **Saitoh, Y., and U. K. Laemmli.** 1994. Metaphase chromosome structure: bands arise from a differential folding path of the highly AT-rich scaffold. Cell **76:**609–622.
49. **Schweizer, D.** 1981. Counterstain-enhanced chromosome banding. Hum. Genet. **57:**1–14.
50. **Selig, S., K. Okumura, D. C. Ward, and H. Cedar.** 1992. Delineation of replication time zones by fluorescence in situ hybridization. EMBO J. **11:** 1217–1225.
51. **Shizuya, H., B. Birren, U. J. Kim, V. Mancino, T. Slepak, Y. Tachiiri, and M. Simon.** 1992. Cloning and stable maintenance of 300-kilobase-pair fragments of human DNA in Escherichia coli using an F-factor based vector. Proc. Natl. Acad. Sci. USA **89:**8794–8797.
52. **Sinnett, D., A. Flint, and M. Lalande.** 1993. Determination of DNA replication kinetics in synchronized human cells using a PCR-based assay. Nucleic Acids Res. **21:**3227–3232.
53. **Sternberg, N. L.** 1992. Cloning high molecular weight DNA fragments by the bacteriophage P1 system. Trends Genet. **8:**11–16.
54. **Subramaniam, P. S., D. L. Nelson, and A. C. Chinault.** 1996. Large domains of apparent delayed replication timing associated with triplet repeat expansion at FRAXA and FRAXE. Am. J. Hum. Genet. **59:**407–416.
55. **Tenzen, T., T. Yamagata, T. Fukagawa, K. Sugaya, A. Ando, H. Inoko, T. Gojobori, A. Fujiyama, K. Okumura, and T. Ikemura.** 1997. Precise switching of DNA replication timing in the GC content transition area in the

human major histocompatibility complex. Mol. Cell. Biol. **17:**4043–4050.
56. **Vassilev, L., and G. Russev.** 1988. Purification of nascent DNA chains by immunoprecipitation with anti-BrdU antibodies. Nucleic Acids Res. **16:**10397.
57. **Vassilev, L. T., W. C. Burhans, and M. L. DePamphilis.** 1990. Mapping an origin of DNA replication at a single-copy locus in exponentially proliferating mammalian cells. Mol. Cell. Biol. **10:**4685–4689.
58. **Warburton, D., S. H. Shaw, T. C. Matise, S. Kalachikov, and S. Fischer.** 1996. Report of the Third International Workshop on Human Chromosome 13 Mapping 1995. Cytogenet. Cell Genet. **75:**85–110.
59. **White, A., J. Tomfohrde, E. Stewart, R. Barnes, D. Le Paslier, J. Weissenbach, L. Cavalli-Sforza, L. Farrer, and A. Bowcock.** 1993. A 4.5-megabase yeast artificial chromosome contig from human chromosome 13q14.3 ordering 9 polymorphic microsatellites (22 sequence-tagged sites) tightly linked to the Wilson disease locus. Proc. Natl. Acad. Sci. USA **90:**10105–10109.
60. **Yandell, D. W., and T. P. Dryja.** 1989. Detection of DNA sequence polymorphisms by enzymatic amplification and direct genomic sequencing. Am. J. Hum. Genet. **45:**547–555.
61. **Zimmermann, K., and J. W. Mannhalter.** 1996. Technical aspects of quantitative competitive PCR. BioTechniques **21:**268–279.
62. **Zoubak, S., O. Clay, and G. Bernardi.** 1996. The gene distribution of the human genome. Gene **174:**95–102.